Arab J Geosci (2010) 3:459–475
DOI 10.1007/s12517-010-0237-8

ORIGINAL PAPER

New constrains on the thickness of the Semail ophiolite in the Northern Emirates

Charles Naville · Martine Ancel · Paul Andriessen · Patrice Ricarte · François Roure

Received: 6 April 2010 / Accepted: 2 November 2010 / Published online: 19 November 2010

Abstract Near-critical angle and refraction studies were performed at IFP as piggyback studies during a wider programme of crustal imagery operated by WesternGeco on behalf of the Ministry of Energy of the United Arab Emirates. The main objective is to illuminate the base of the Semail Ophiolite along part of a regional transect (D1) crossing the Northern Emirates from the Gulf of Oman in the east up to the Arabian Gulf in the west. Results confirm that the sole thrust of the ophiolite has been folded during the Miocene stacking of the underlying Arabian Platform. The thickness of the ophiolite grades from zero in the core of the Masafi tectonic window, up to a maximum of 1.7 km below the axial part of a successor basin which has been preserved on top of the serpentinite west of the current exposure of the main ultramafic bodies. Apatite grains extracted from plagiogranites of the Semail ophiolite also provide evidences for an early unroofing of the gabbros and plagiogranites during the Late Cretaceous, with cooling ages of 72–76 Ma at the top of the ophiolite in the east (not far from the Fujairah coast line), which are coeval and also consistent with the occurrence of Late Cretaceous paleo-soils, rudists and paleo-reef deposits on top of serpentinized ultramafics in the west. Younger cooling ages of 20 Ma have been also found at the base of the ophiolite near Masafi, in the core of the nappe anticline, thus providing a Neogene age for the refolding of the allochthon and stacking of underlying parautochthonous platform carbonate units. These results, together with the occurrence of a thick sedimentary pile illuminated below the metamorphic sole along the north-trending, strike-profile D2 running parallel to the axis of the Masafi window, should stimulate a renewal of the exploration in the central part of the Emirate foothills, where the ophiolite thickness is currently limited, and was already drastically reduced by the end of its Late Cretaceous obduction.

Keywords Semail ophiolite · Refraction seismic · Critical angle · Critical reflection · Surface seismic

C. Naville (✉) · M. Ancel · P. Ricarte · F. Roure
Geology-Geochemistry-Geophysics, IFP Energies nouvelles,
1 et 4, Avenue de Bois-Preau - BP 311,
92852, Rueil Malmaison Cedex, France
e-mail: Charles.Naville@ifpenergiesnouvelles.fr

M. Ancel
e-mail: Martine.ANCEL@ifpenergiesnouvelles.fr

P. Ricarte
e-mail: Patice.Ricarte@ifpenergiesnouvelles.fr

F. Roure
e-mail: Francois.Roure@ifpenergiesnouvelles.fr

P. Andriessen · F. Roure
Faculty of Earth and Life Sciences, VU University,
de Boelelaan 1085,
1081, Amsterdam, The Netherlands

Introduction

Petroleum exploration is usually limited to passive margins and foreland basins, or to the outer part of foothill areas despite the fact that they are usually considered as frontier zones for exploration due to the increasing risk there to drill a dry hole. For instance, for many years seismic imagery was not able to illuminate the part of sedimentary basins which is currently buried beneath high velocity screens such as volcanic flows and peridotites. Because ophiolites are assumed to represent part of or the entire oceanic crust and upper part of the mantle of former oceanic lithospheric plates, and are commonly associated with either high pressure–low temperature (blueschist facies) or high pressure–high temperature (amphibolite facies) metamorphic

K. Al Hosani et al. (eds.), *Lithosphere Dynamics and Sedimentary Basins: The Arabian Plate and Analogues*, Frontiers in Earth Sciences,
DOI: 10.1007/978-3-642-30609-9_3, © Springer-Verlag Berlin Heidelberg 2013

sole, zero or very limited petroleum exploration has been yet initiated beneath the Mirdita Ophiolite in the central foothills of Albania, nor under the Semail Ophiolite which crops out in the Northern Emirates and in the adjacent parts of Oman. Nevertheless, improvements of seismic imagery and better estimates on the timing of erosional unroofing by means of paleo-thermometers provide new ways to properly predict the paleo-burial and coeval paleotemperature reached by reservoirs and source rocks associated with the lower plate below the ophiolite (Muceku et al. 2007; Roure et al. 2010a, b), and therefore, to better evaluate the exploration risk in such challenging, yet unexplored frontier areas. In this context, results of an integrated geophysical and geological survey of the Northern Emirates are discussed below to document our understanding on both the current thickness of the Semail Ophiolite west of the Masafi tectonic window, and on the timing of its erosional unroofing history.

New geophysical data used for this study include a complete aeromagnetic coverage performed by Fugro, and four deep seismic profiles also recently recorded by WesternGeco on behalf of the Ministry of Energy of the United Arab Emirates (Styles et al. 2006; Fig. 1), two of them running east–west from the Gulf of Oman in the east up to the Arabian Gulf in the west (profiles D1 and D4), the two other being trending north, one in the foreland (profile D3), the other one in the ophiolitic and metamorphic, inner part of the Oman Range (profile D2).

Petroleum exploration is indeed becoming mature in the Arabian foreland, and gas-condensate fields of Margam and Sajaa (Blinton and Wahid 1983; Alsharhan 1989; O'Donnell et al. 1994; Fig. 1) already demonstrate the exploration potential of the frontal part of the Northern Emirates foothills. Therefore, further challenges for the exploration now relate to the depth, thickness and thermal evolution of sedimentary layers which are still present in the parautochthonous Arabian Platform units currently underthrust or stacked within the lower plate, east of the Late Cretaceous and Miocene fronts of deformation. Despite the fact that coupled geophysical, paleo-thermometers and further basin modelling studies were able to answer these questions; this paper focuses only on the upper plate, i.e. the current and past thickness of the ophiolite. Two companion papers (Tarapoanca et al. 2010; Callot et al. 2010) will provide more details on the kinematic, burial and fluid flow history of the lower plate, as evidenced by Thrustpack and Ceres 2D modelling, whereas further geophysical processing data and petroleum results of the project, i.e. thermal modelling and simulations of potential source rock maturation and hydrocarbon migration can be found in the publications of the Ministry of Energy of the UAE (Naville et al. 2006; Roure et al. 2006).

Regional geological background

The Oman Range constitutes the back bone of the northeastern Arabian corner, extending from the central and northern part of the Sultanate of Oman in the south, up to the Hormuz Strait in the north. A relatively wide portion of the foothills is located in the Emirates, i.e. in the vicinity of Al Ain in the Abu Dhabi Emirate, in the vicinity of the Sajaa and Margham gas-condensate fields in Sharja and Dubai emirates, as well as in Ras-Al-Kaimah Emirate farther to the north, whereas a limited part of the inner, ophiolitic part of the range extends in the Fujairah Emirate, between the Musandam Peninsula and the Dibba Zone in the north, and the political border with the Sultanate of Oman in the south (Styles et al. 2006; Fig. 1).

The Semail Ophiolite constitutes a fragment of oceanic lithosphere which has been obducted in Late Cretaceous times on top of the adjacent Arabian passive continental margin (Coleman 1981; Goffé et al. 1988; Le Métour et al. 1990; Searle and Cox 1999; Gray et al. 2000). Wide tectonic windows exist in the Sultanate of Oman, i.e. in the Jebel Akhdar (Rabu 1987; Breton et al. 2004), where even the Paleozoic to Mesozoic series of the Arabian Platform is widely exposed beneath the ultamafic rocks. Farther north, only the shallower parts of the tectonic pile, made up of the far-travelled Hawasina basinal units and the metamorphic sole of the ophiolite (Ghent and Stout 1981; Lanphere 1981; Michard et al. 1982; Searle and Malpas 1980, 1982; Lippard 1983; Gnos and Peters 1993; Gray and Gregory 2000) are documented below the Semail Ophiolite. The refolded attitude of many thrust planes and the surface distribution of the main lithostratigraphic units allowed already to propose a representative cartoon summarising the vertical and lateral distribution of the main tectono-stratigraphic units across an idealised transect in the Northern Emirates (Fig. 2), hypothesising the occurrence of a wide underthrusting of the former Arabian passive margin beneath the far-travelled basinal and ophiolitic assemblage.

The entire oceanic crust, including gabbros, sheeted dykes, pillow lavas and deep water sediments, is still preserved in the southern part of the Semail Ophiolite in the Sultanate of Oman, whereas mainly the lower part of the oceanic crust, i.e. the gabbros, is still preserved in the eastern part of Fujairah. Further west, only fragments of the former oceanic mantle, made up dominantly of serpentinized peridotites, are still preserved in the Northern Emirates. Worth to mention, the metamorphic sole of the ophiolite also is exposed in the Masafi tectonic window

Apart of surface outcrops, the regional extent of the Semail Ophiolite is well constrained by the magnetic survey performed by Fugro (Ministry of Energy of the UAE 2006):

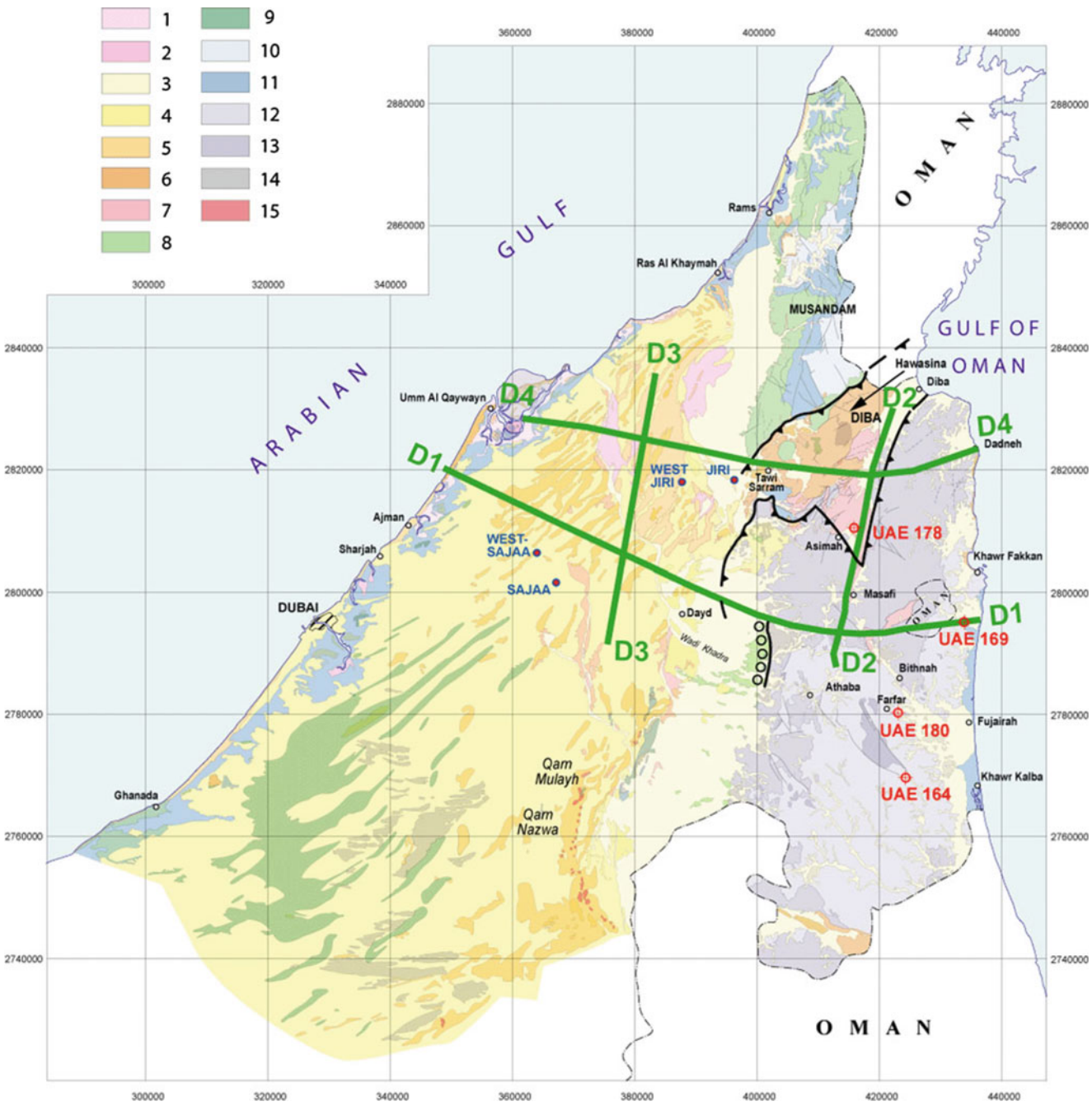

Fig. 1 Geological map of the Northern Emirates, outlining also the location of the deep seismic profiles and apatite fission–tracks samples

– 1. To the west, serpentinized peridotite becomes progressively buried along profile D1 beneath thick post-orogenic coarse clastic series;
– 2. To the east, in the proximal Fujairah offshore domain, shallow ophiolitic bodies still account for a strong magnetic anomaly, whereas the oceanic crust is either absent or become too deep farther east to be identified in the distal Fujairah offshore by means of remote sensing or by conventional reflection seismic.

As evidenced by refraction seismic, the peridotite is probably strongly serpentinized along profile D1, west of D2, thus accounting for velocities as low as 5 km/s, whereas massive peridotite still averages 6 km/s east of D2.

Total thickness of the ophiolite is far from constant in the foothills, the sole thrust of the Semail unit being clearly refolded, as evidenced by the occurrence of the Masafi tectonic window, where the underlying metamorphic sole of the ophiolite is exposed at the surface (Fig. 1). Along profile D1, the ophiolite can be subdivided into two distinct

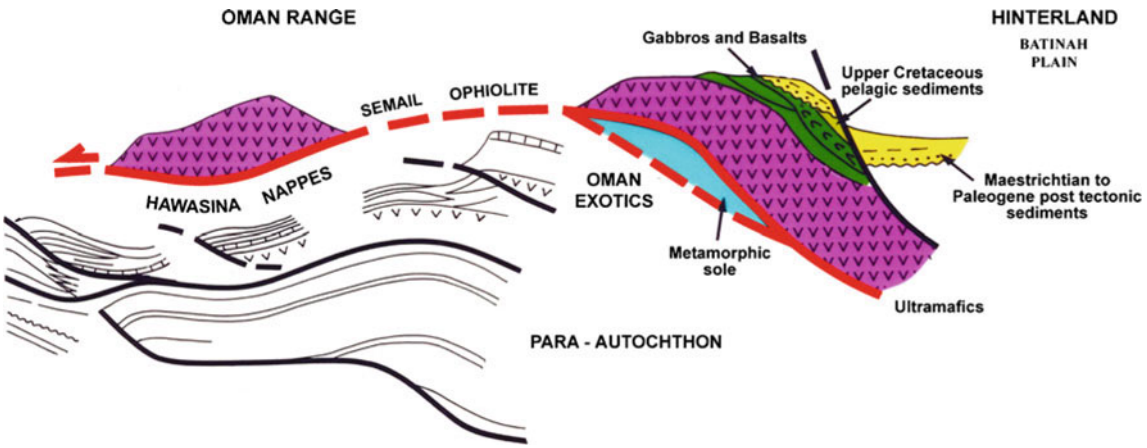

Fig. 2 Conceptual sketch outlining the main tectono-stratigraphic units involved in the foothills of the Northern Emirates. *Top* Lower Cretaceous platform carbonates of the lower plate, comprising both the autochthonous Arabian foreland and parautochthonous units currently underthrust beneath the Hawasina-Sumeini basinal allochthon, are outlined in *green*. *Bottom* the upper plate comprises the Semail Ophiolite (*purple*) and its metamorphic sole (*blue*). Notice that both the upper plate, made up of the Semail Ophiolite, and the intermediate plate, which is made up of the Hawasina-Sumeini allochthon (*white*), have been refolded during the Neogene stacking and out-of-sequence thrusting of parautochthous platform units of the former Arabian passive margin

domains: (1) a relatively thin one west of D2(Aswad block), where the ophiolite is less than 2-km thick and (2) a thicker one east of D2 (Fakkan block), up to 4–5-km thick according to Fugro interpretation of aero-magnetic data (Styles et al. 2006).

Due to the lack of seismic reflection from standard processing output at the transition between offshore and onshore Fujairah, and because offshore reflection data do not image even the base of the sediments, the precise architecture of the eastern part of the Semail unit still remains underconstrained. Refraction and near-critical reflection processing procedures still need to be attempted on line D2 and on the eastern part of D1 and D4 lines. In our interpretation, we consider that the Semail allochthon has been locally back-thrusted toward the east in the vicinity of the coast line, the surface trace of this thrust being actually outlined by the easternmost extent of the magnetic anomalies on Fugro maps.

Specific seismic imaging of the ophiolite base by near-critical offset refraction stack and near critical incidence reflection stack

Four deep seismic profiles have been recorded by Western-Geco for the Ministry of Energy, UAE, in the aim to delineate the vertical extent of the ophiolite. The location maps of the deep reconnaissance survey appear in Fig. 1

Complementary geophysical studies have been carried on the long offset traces (up to 15 km), i.e. first arrival tomography applied to the eastern part of profile D1, and using the seismic refraction method and near-critical incidence reflections on the test line indicated on Fig. 3a. The large offsets, high source energy and main field acquisition parameters used for this survey are summarised on Fig. 3b.

The high refraction velocities observed around 6 km/s very near surface over the ophiolite outcrops and at relatively short offset distance can be associated with the top of a high-velocity formation corresponding either to the base of ophiolite layer, or equally to the base of the metamorphic sole, roughly 100 m deeper (an estimation from outcrop observations). The near-offset refraction

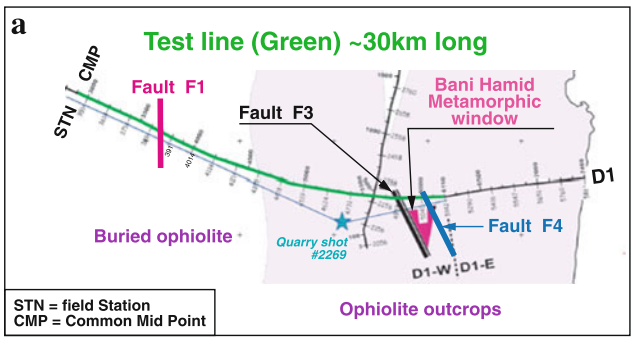

Test line for base ophiolite imaging, with quarry shot geometry

b

Vibroseis Reflection with 1600 live traces, 25m apart

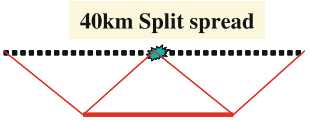

Source:
8 vibrators, 60,000 lbs each, 60%drive
Sweep: 6-48Hz, 4 sweep/VP/25m
20s length + 20s listening.
Recorder Sercel SN388: 4ms,
Diversity stack-8 BEFORE correlation

Main field acquisition parameters.

Fig. 3 **a** Location map of the test study line for base ophiolite imaging. **b** Main field acquisition parameters

velocities are about 5 km/s on the ophiolite outcrops. For lack of better identification, the buried 6 km/s refraction marker will be referred to as "ophiolite base" in the present paper, although the matter will be briefly analysed in the "Discussion" section.

The preliminary examination of raw seismic records indicated that the refraction method would allow tracing the base of the ophiolite between the western foothills and the Bani Hamid tectonic window (Fig. 3), where the infra-ophiolitic metamorphic sole is exposed. Because the peridotites have been deeply serpentinized west of Masafi, their seismic velocity averages only 5 km/s (varying from 4.4 to 5.3 km/s), which is slightly lower than underlying carbonate units derived from the former Arabian margin with velocity up to 6 km/s. The absence of zero-incidence reflection on the interface between the ophiolite and underlying carbonates, accompanied with a strong reflection amplitudes near critical angle, may be explained by an exact inverse contrast in velocity and density at that interface: if so, the density of the ophiolite could be estimated to a maximal value about 3 g/cm^3, versus 2.6 g/cm^3 for the carbonates, while the velocity increases from 5 to 6 km/s, respectively.

Preliminary observations details and illustrations

Note: the time scale unit is in second, on all time series represented on Figs. 4, 5, 6, 7, 8, 9, 10, 11 and 12; the stack sections on Figs. 11 and 12 are in two-way time scale (twt)

- *Outcropping ophiolite rocks: field stations (STN) # 4355–5142 on test line, at the end of D1-W*: Fig. 4 shows the raw data from VP#4500, corrected with 5 and 6.0 km/s velocity linear move out (LMO, or in "reduced times" after X/V correction). The top display shows that the effective ophiolite velocity value is about 5 km/s, as the direct arrivals propagated on the ophiolite outcrops appear aligned on the front and rear spreads (intercept peak time 80 ms), the cross-over offset with the direct arrival in the weathered zone being very short, around 100 m offset.

  The bottom display illustrates how the base–ophiolite marker appears dipping westward, confirmed by a small intercept time (200 ms) and short 4 km cross-over distance on the front spread (right side), in contrast with a large intercept (~950 ms) and large offset of apparition in first arrival (>13 km) on the western side (left).
- *Buried ophiolite stations # 3720–4355*: The ophiolite rocks are cropping out beyond station #-4355 eastward. Figure 5 shows the raw data of VP # 4020, corrected with 5 and 6.5 km/s velocities.

  On the top display, one can definitely assess the velocity of the ophiolite around 5 km/s, as the top-ophiolite head-wave arrivals appear around the 2 km (80 stations) cross-over offset, and are aligned on the front and rear half spreads (intercept time 0.6 s), in conjunction with the very high reflection amplitudes of the top ophiolite interface (0.55 s twt). Beyond critical incidence offset of about 1.5 km (60 stations), the strong wide angle top-ophiolite reflection typically appears with the velocity of the Tertiary overburden, around 2 km/s. The top-ophiolite refraction marker is abruptly interrupted westward around station #3780,

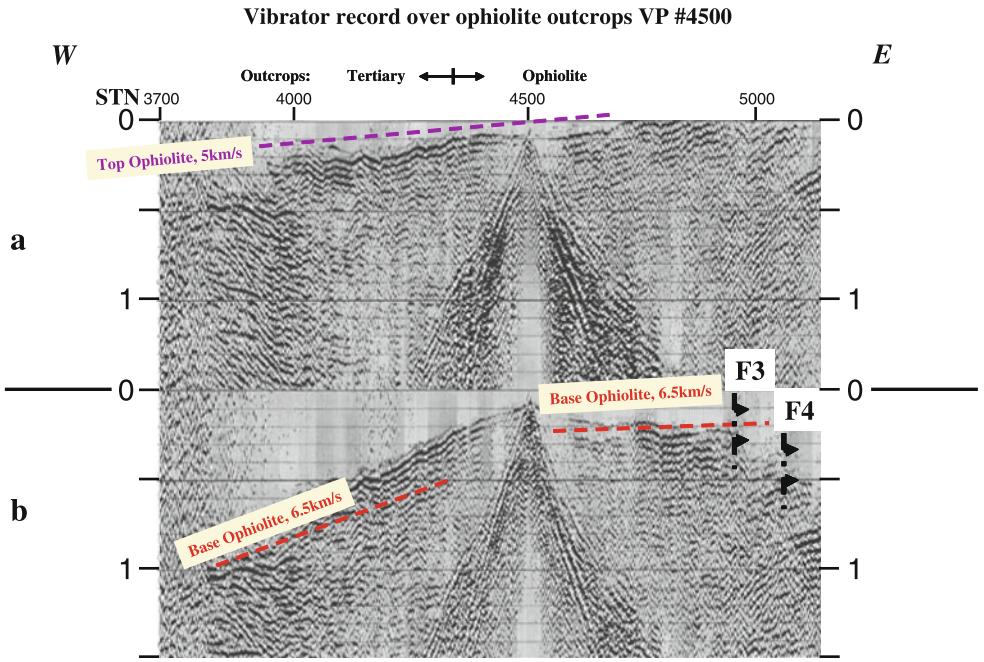

Fig. 4 Vibrator record over ophiolite outcrops, VP #4500, LMO-corrected 5, 6 km/s

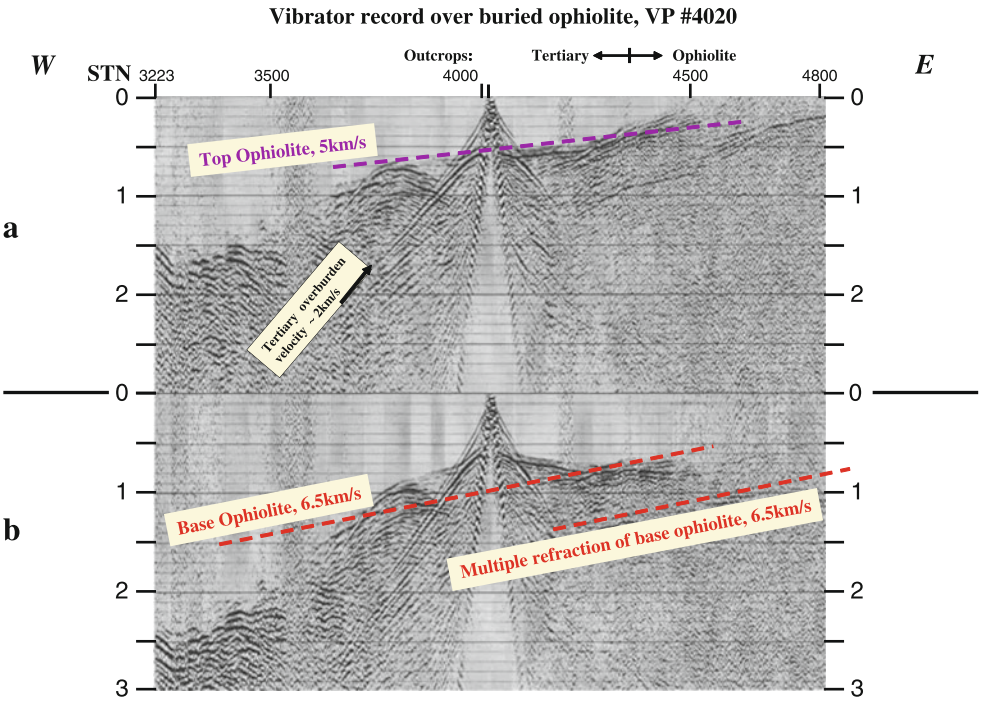

Fig. 5 Vibrator record over buried ophiolite, VP #4020, LMO-corrected 5, 6 km/s

where a spectacular diffraction occurs with forward and back scattering (apex at station #3780)

On the bottom display, a deeper, faster refraction marker can be identified around 1.0 s intercept time, with a 6.5 km/s velocity. Westward, an abrupt lateral interruption of the refracted arrival is marked by high-energy diffraction with apex located between station #3760 and station #3860. On the western half spread, beyond 11 km offset, from station #3223 to station #3570, a major deepening of the fast 6–6.5 km/s velocity formations propagating the refracted arrivals is observed. Thus, two major structural compartments are observed in line D1: a low-velocity sedimentary basin in the west of station #3700 approximately, and a high-velocity compartment eastward. On the eastern front spread, the cross-over between top and base ophiolite refracted arrivals is clearly located around station #4300, 7 km from VP #4020. The similar high velocity found for the shallow and outcropping formations on line D2 indicates that this 6.5 km/s refraction marker corresponds to the compacted and massive limestone formations underlying the ophiolite layer. Consequently, it will be referred to as the "base-ophiolite" refraction marker.

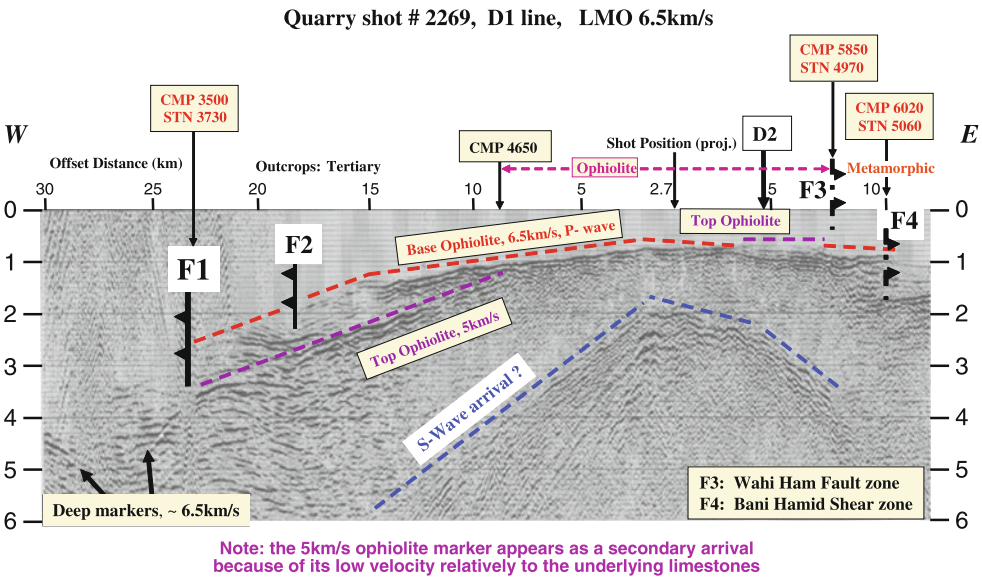

Fig. 6 Quarry shot #2269, D1 line, LMO-corrected 6.5 km/s

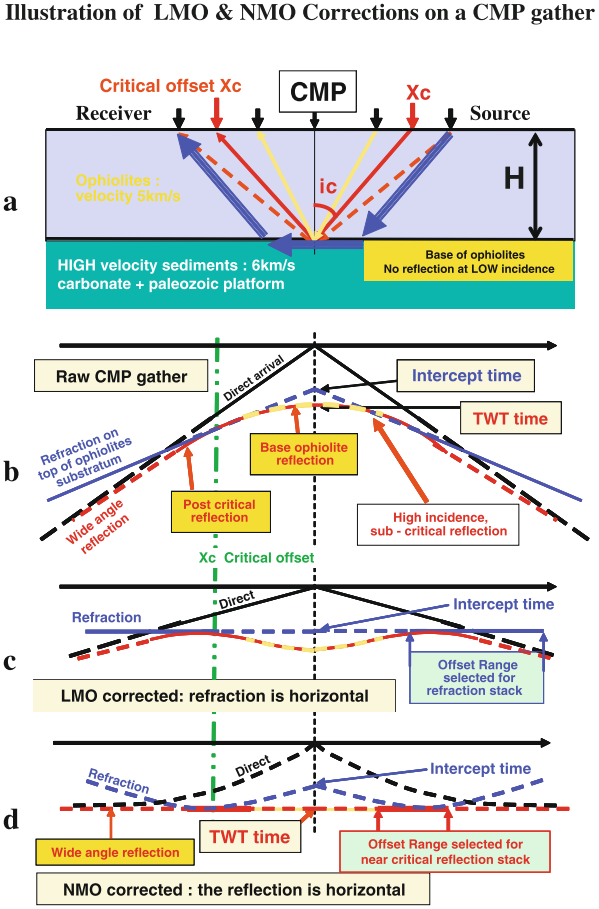

Fig. 7 Illustration of LMO and NMO corrections on a CMP gather: **a** ray sketch, **b** raw CMP gather, **c** LMO corrected, **d** NMO corrected

Interestingly, on the eastern half spread, a late refracted arrival can be followed in secondary arrival, parallel to the fast base-ophiolite head-wave, with a 500-ms delay possibly related to a multiple arrival generated between top ophiolite with the surface.

Both head-wave arrivals are totally attenuated beyond station #4480 eastward (11 km offset about). The total extinction of the head-waves beyond 10–12 km offset can be observed on many successive seismic records in this zone. Beyond 11 km offset, delayed head-waves appear, due to a deeper penetration of the refracted propagation. A similar "diving wave effect" in thick multilayered limestone can be commonly seen on records of line D2 and east D4.

- *Remark on refraction seismic analysis*: The interruption of a refraction marker can be generated by either a real fault, or by an erosion cliff for instance, this is the reason why an undefined refraction marker interruption is referred to as an "accident".
- *Quarry blasts on line D1:* Figure 6 shows the shot #2269, LMO corrected with 6.5 km/s velocity, labelled with the receiver number and offset distance (m). This shot is located 2.73 km laterally to the receiver line (location map in Fig. 3a), so that it illuminates large segments of the base ophiolite marker. Common mid-point (CMP) #4650 corresponds to the western limit of the ophiolite outcrops. The buried ophiolite corresponds to the marker underlined in magenta colour on Fig. 6, and appears as a secondary arrival because the ophiolite velocity (5 km/s) is lower than the underlying limestone velocity (6.5 km/s). The western limit of the buried ophiolite is marked by a major accident F1, accompanied by a probable change in the nature of the refraction marker as a spectacular deepening of the fast velocity formation is observed westwards, amounting to about 0.8 s in intercept variation (or near 2 s in two-way reflection time). On the east side of accident F1, the record of quarry shot #2269 directly confirms the thinning of ophiolite layer towards east, updipping at least up to the D1/D2 line crossing, and possibly further east.

The above preliminary observations indicate that the 6–6.5 km/s base of ophiolite refraction marker can be followed by the Gardner method applied to vibroseis records (Gardner 1939), as no reflection has ever been seen during the standard stack tests and velocity analysis run by WesternGeco over the outcropping ophiolite. Indeed, the common reflection imaging technique takes in account only a lower than critical incidence angle range. The application of the long range refraction method is based on the notion of "refraction marker", characterised by specific wave shape of first head-wave arrival associated with distinguished velocity for each marker: when this is observed, the corresponding geological horizons can be tracked and mapped.

The first arrival tomography inversion was tested. This method takes into account only the arrival times and assumes a velocity model with smooth velocity gradient, appropriate to the propagation of diving or turning waves. Unfortunately for the interpreter, the results of the first-arrival tomography were not convincing enough to ensure that the new velocity model would result in a significantly improved pre-stack depth migration, or in any significant improvement leading to new geological insights.

Therefore, it was decided to proceed with refraction and high incidence/wide angle reflection processing attempts in order to tentatively glean additional structural information. Since line D1 was acquired with a heavy vibrator source/short 25-m interval (Fig. 3b), over a large range of source to receiver offsets, and due to time constraints, the conventional Gardner refraction method using time picking has

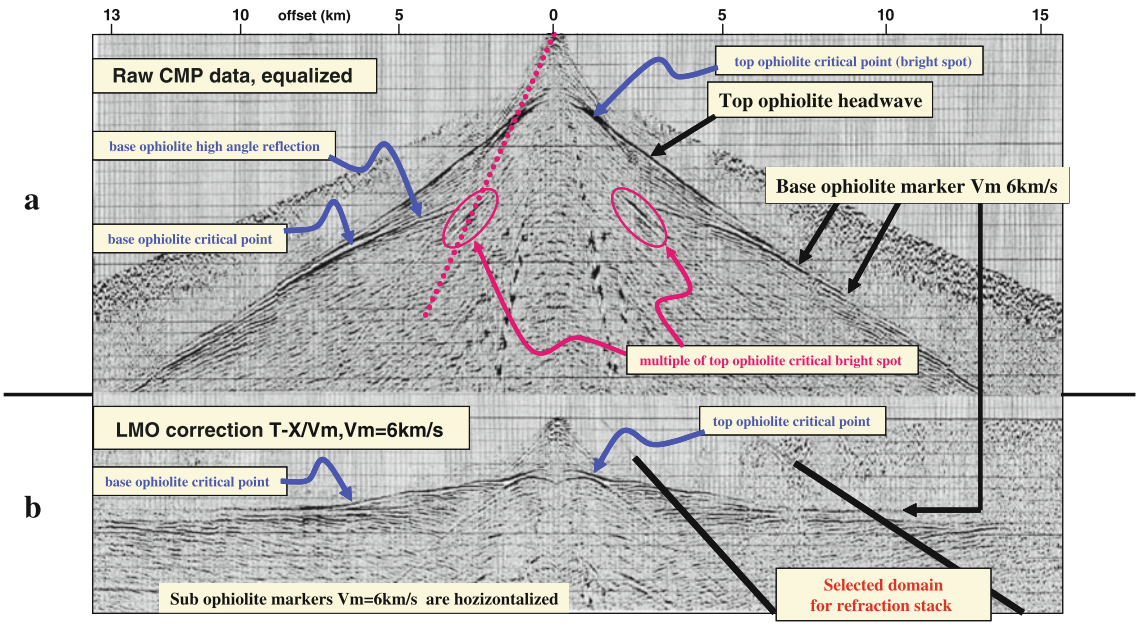

Fig. 8 CMP gather #4040 over buried ophiolite: **a** raw data (*top*), **b** LMO corrected 6 km/s (*bottom*)

been left aside. Instead, a quicker attempt of continuous near critical angle refraction stacking, inspired by the "Constant Distance Correlation" method (Clément and Layat 1961), appeared as a more direct imaging solution taking into account the existence of ready-made pre-processed data in CMP collections, the present capabilities of the modern seismic software and the acquired practise of the seismic reflection processors.

Refraction stack inspired by the "Constant Distance Correlation" method

The "Constant Distance Correlation" method (Clément et al. 1961; Layat 1967) is an original approach towards the industrialisation of the refraction method, taking advantage of the high amplitudes observed at near-critical angle, in order to map a refraction marker precisely, while minimising the source energy effort to obtain a good signal to noise ratio at large offset. In addition, the industrialisation of the Gardner refraction processing attempted in the early times of digital processing (Péraldi and Clément 1972) is still attractive and inspiring in the cases where the reflection seismic method fails to yield satisfactory images, while clear head wave arrivals are observed.

The near-critical incidence refraction arrival and high-angle/near-critical angle reflection arrivals are illustrated on Fig. 7, representing a CMP gather of seismic signals. Figure 7a is a sketch of the seismic rays with common mid-point, in a two-velocity, horizontal layer medium. Critical offset and incidence are respectively noted *Xc* and *ic*. Reflected rays are drawn up to critical incidence, and refracted ray (blue) beyond.

The reflected event (solid red line-up) is illustrated as it appears on the data sorted as a CMP gather in different configurations of time corrections, as follows: raw-time CMP collection (Fig. 7b), Linear move out (LMO) corrected at refraction velocity, or velocity of the fast substratum (Fig. 7c), and Normal move out (NMO) corrected with the exact stacking velocity or rms velocity of the overburden layer (ophiolite+tertiary) above the concerned interface (Fig. 7d).

The offset range selected for refraction stack is indicated on the LMO-corrected middle display; the offset range selected for the high-angle reflection stack is indicated on the NMO-corrected bottom display. The criterion for insuring the accurate LMO or NMO correction velocity remains the horizontal aspect of the corrected event before stacking.

Figure 8 represents the CMP gather #4040 pre-processed data collection, located over the buried ophiolite, in raw times (top, Fig. 8a) and in reduced time, filtered (bottom, Fig. 8b), equalised over a 1-s long sliding window. This display clearly shows the reflection and refraction arrivals of the top ophiolite interface, as well as the critical point. Pre-critical and post-critical reflection arrivals of the top ophiolite reflection are distinct. A notable multiple of the critical bright spot of the top ophiolite seismic interface clearly appears at twice the time, twice the offset of the critical point; which accounts for the generation of refraction multiples at larger offset distance.

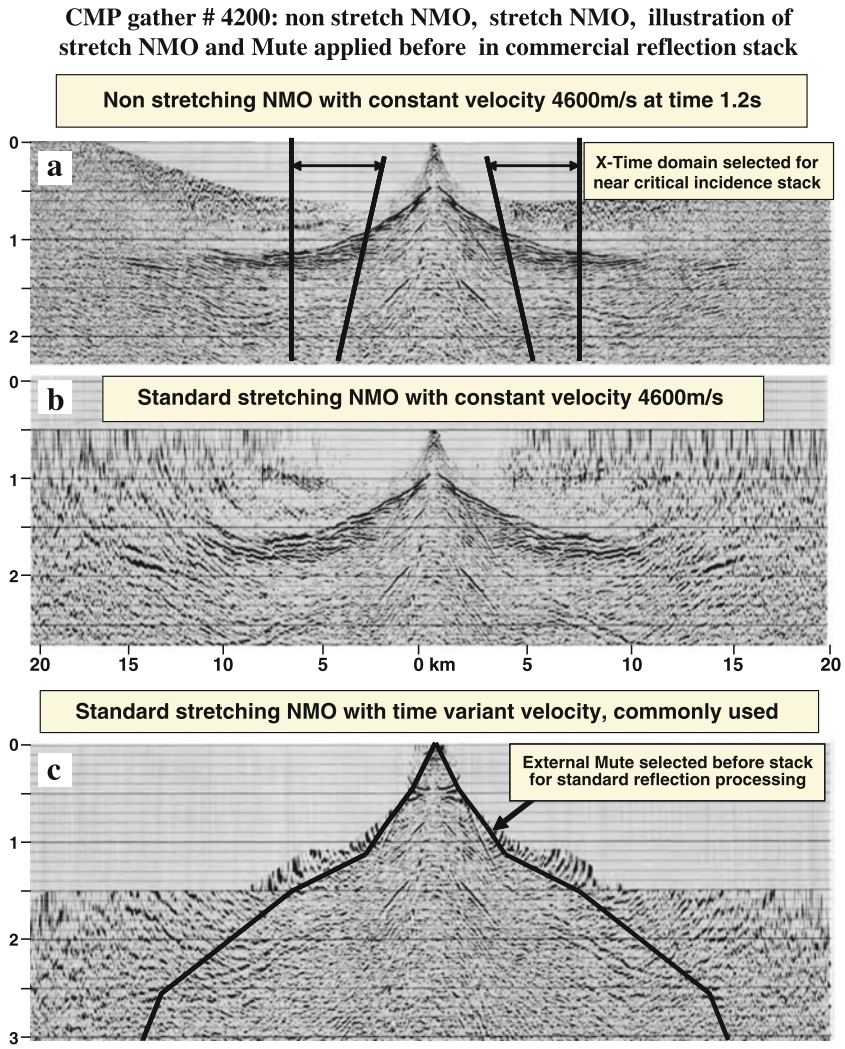

Fig. 9 CMP gather #4200 over buried ophiolite: **a** stretch less NMO 4.6 km/s at 1.2 s twt (*top*), **b** standard stretch NMO at constant velocity 4.6 km/s for all times twt (*centre*), **c** standard stretch NMO at time variant velocity and Mute applied before stack in commercial processing (*bottom*)

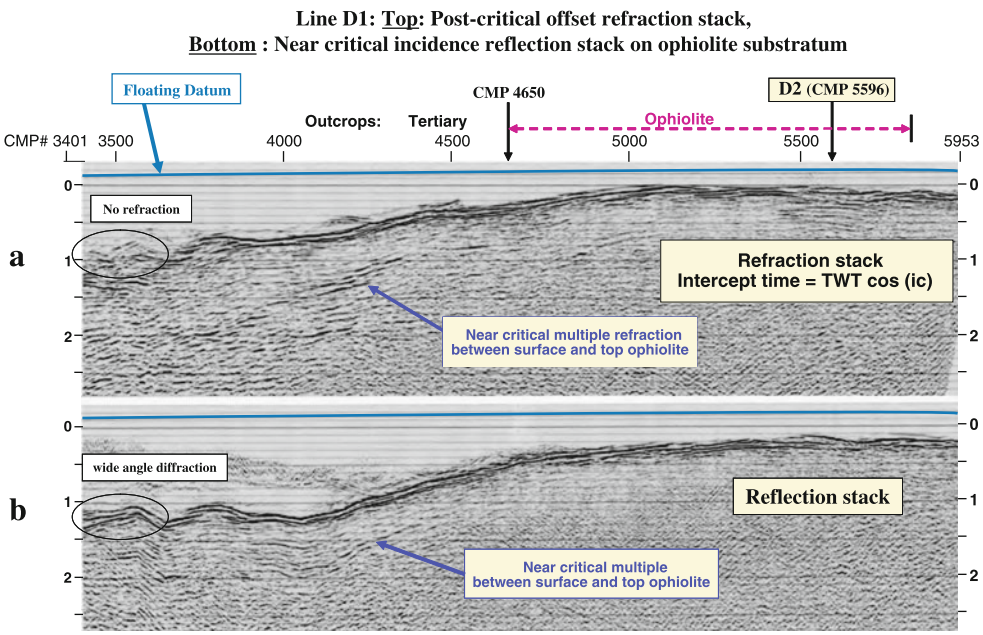

Fig. 10 Line D1: **a** critical to post-critical offset refraction stack (*top*). **b** Near-critical incidence reflection stack on ophiolite substratum (*bottom*)

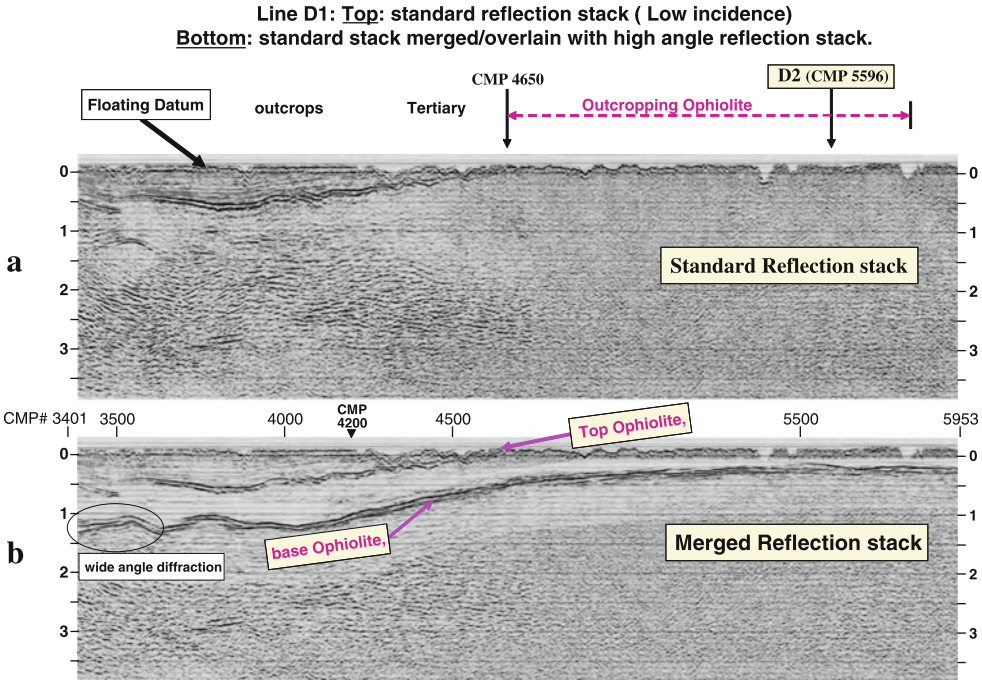

Fig. 11 Line D1: **a** standard, low-incidence reflection stack (*top*). **b** standard stack merged/overlain with high-angle reflection stack (*bottom*)

The base ophiolite seismic interface is nicely marked by the high amplitudes observed near the critical point (about 5 km offset), by the 6 km/s refraction head-wave, and by the immediate high incidence pre-critical reflection arrival. The desired base ophiolite reflection event appears on Fig. 8a as a hyperbolic line-up in a limited offset range immediately inferior to the critical offset. The base ophiolite low incidence reflection is remarkably absent. Beyond 6 km offset, the first arrival corresponds to the high velocity (6 km/s) refraction on the top of the formation immediately underlying the ophiolite.

The bottom display (Fig. 8b) in reduced time, obtained after 6 km/s LMO correction, clearly shows the sub-ophiolite refraction marker aligned in horizontal position. The time-offset domain between the solid slanted black bars (Fig. 8b) was retained to build the refraction stack presented on Fig. 10a (top), in intercept time scale from the same near-surface floating datum as the standard reflection stack.

Comments on near-critical refraction stack presented on Fig. 10a The excellent results shown by the seismic refraction stack demonstrate the possibility to map continuously the base of the thrusted ophiolite layer.

The 6 km/s top of ophiolite substratum marker appears as a quite rugged surface below the buried ophiolite, with

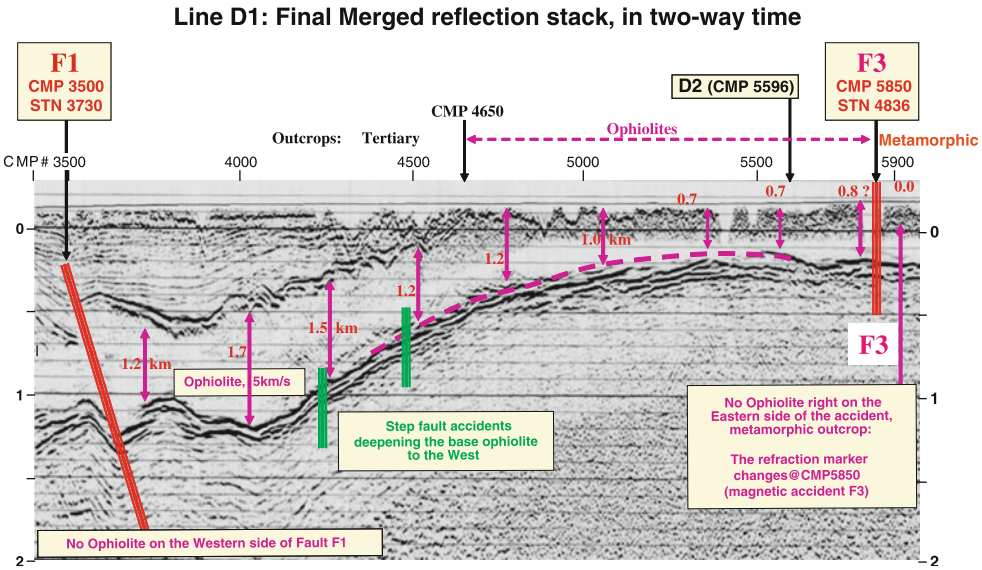

Fig. 12 Line D1: final merged reflection stack, in two-way time, commented

probable faults (CMP #4100, 4200) which are possibly accompanied by limited westward thrusts.

The western end of the refraction stack shows a sudden interruption of the 6 km/s marker around CMP #3600, associated either to the extremity of the ophiolite sheet, or to a major geological accident.

The interpreter of the refraction stack on Fig. 10a (top display) need to be reminded that only the horizon representing the base ophiolite interface can be read with confidence on this document. The coherent line-up appearing at later time below the western buried ophiolite section likely represents a multiple of refraction events, probably generated by the base of weathered zone with the strong top of ophiolite reflecting interface.

At the eastern end, the refraction image stops around CMP #6000 due to the fact that line D1-west was recorded with the last geophone group at the position of CMP #6100. The refraction image can be obtained only up to a single refraction offset distance (2.5 km) before CMP #6100.

High-incidence angle reflection stack using appropriate NMO correction and mute of pre-processed CMP data collections

In the central-eastern part of D1 where the ophiolite is buried, its base can clearly seen in reflection at high, near-critical incidence angle, as illustrated by CMP gather #4040, Fig. 8.

A few CMP collections have been examined in order to evaluate the NMO velocity to be applied, and to select the time–offset domain of the base ophiolite event to be stacked. Figure 9a–c show the CMP #4200 collection, located over the buried ophiolite, with the following time corrections:

- CMP gather after application of a non-standard/non-stretching NMO correction with constant velocity 4,600 m/s, focussed on the ophiolite base reflection only (Fig. 9a);
- after application of the standard stretching NMO correction with constant velocity 4,600 m/s (Fig. 9b);
- after application of the standard stretching NMO correction with time variant velocities retained for the standard processing, superimposed with the narrow mute selected prior to the contractor standard stack (Fig. 9c).

Therefore, it appeared appropriate to attempt producing a high-incidence angle reflection stack image, which would be easier to build and more precise than high-quality refraction images. As the standard NMO correction procedure induced damaging stretching effects at high incidence (Fig. 9b, c), and as the velocity analysis were delicate, possibly due to additional layering anisotropy effects in the vertical plane, a non-stretching/non-standard NMO procedure, aimed at correcting only the base ophiolite reflector was retained to preserve the base ophiolite reflection event at high incidence. Thus, the time–offset domain between the solid slanted black bars (Fig. 9a) was selected to build the high incidence reflection stack presented on Fig. 10b (bottom), in two-way time scale, from the same floating datum origin as the standard reflection stack.

Comments on the high-incidence reflection stack presented in Fig. 10b Figure 10b (bottom) exhibits the high-incidence reflection stack test on the central part of line D1, using a constant velocity and non-stretching NMO procedure and rough mute before stack aimed to the preservation of large offsets corresponding to immediate pre-critical to critical reflection angles.

Velocities needed to be refined, as well as the mutes, in order to insure a higher reliability of the reflection response, at least for the two way times of the target base ophiolite horizon. The NMO velocities were adjusted by ±10% along the "base ophiolite reflector", in order to yield the most laterally coherent stack (the usual industrial stack enhancement routines improving the NMO velocity through maximisation of stacked energy could not be used in the present non stretching NMO configuration). Additional mute tests and "angle" stacks in narrow successive incidence angle domains are desirable to refine the base ophiolite reflection response.

Moreover, we noticed that in the outcropping ophiolite section, the direct arrivals on the CMP collection data pre-processed by W-G are partially to totally muted in the near-critical offset range, which changes the lateral character of the refraction stack and of the high incidence reflection stack in the same interval (~ CMP #5,000–CMP #5,500).

It looks obvious that more time and attention is needed to refine the mute design and the stacking velocities in order to improve the base ophiolite reflection response.

Very likely, standard processing routines could be applied in order to obtain a reflection section exhibiting both top and base ophiolite horizons.

Possibly deeper reflections could be recovered at high incidence, below the base of ophiolite; however, obtaining a high-quality deep stack image fell beyond the time constraints of the present reconnaissance study.

On Fig. 10, the top part represents the refraction stack, in intercept time, to be compared with the high-incidence reflection stack (bottom part), in two-way time. The two images are very similar, except for the western tip of the base ophiolite layer, where the bottom reflection stack shows high-incidence diffraction, also exhibited by the standard reflection stack on Fig. 11a,

top display, or on Fig. 12 (larger time scale) at about 1.2 s. The reflection two-way stack times are about 30–45% larger than the intercept times, which is in good agreement with the velocity contrast between the overburden from the base ophiolite to the ground level, according to the relationship:

$$\text{Intercept} = \text{TWT}.\cos\left[\text{asin}(\text{Voverburden}/\text{Vmarker})\right] = \text{Twt}.\cos(\text{asin}(5/6)) = 0.55\ \text{Twt}$$

As the high-incidence angle reflection stack is satisfactory over the buried ophiolite section and ophiolite outcrop interval, there is potentially no need for a refraction stack.

Warning! The interpreter should keep in mind that multiple refracted arrivals and multiple near-critical reflection line-ups are prevalent below the base ophiolite horizon on the western half of the sections presented on Fig. 10a, b. Therefore, these events do not represent any true deeper seismic interfaces. The strong observed multiple is likely generated between the top-ophiolite reflector and the surface.

Final results on central line D1

The high-incidence reflection stack, Fig. 10b (bottom) can be accurately compared with the same twt time scale with the standard stack, Fig. 11a (top). Thus, both reflection stacks have been merged on Fig. 11b: a limited time-windowed corridor have been selected along the base ophiolite high-angle reflection horizon, and superimposed over the standard reflection stack section. This superimposition has been done with full precision with the CGG Geocluster software system, after same equalisation on both sections, so as to obtain a single-output section readable in SEG-Y format.

Figure 12 represents an expanded version of the merged stack of Fig. 11b, with indication of the approximate thickness of the ophiolite layer, and major accidents.

- The western tip of the ophiolite is marked by the abrupt extinction of the top and base ophiolite reflectors and of the base ophiolite refraction marker: this extinction has been observed as accident F1 on Fig. 12 at CMP 3500, in field extinction position on Fig. 6. The true position of the western edge of buried ophiolite is located at about CMP 3600, due to the offset observation of the refracted event, and due to the fact that the stack section on Fig. 12c is not migrated. Fault F2 affecting the ophiolite base (Fig. 6), is located right to the east of the base ophiolite western edge (~CMP 3700).
- The eastern tip of the ophiolite is marked by the refraction accident F3 which coincides with a major magnetic accident and with the appearance of metamorphic outcrops eastward (see surface geological map, Figs. 1, 3a and 15). The fact that this accident is not seen on the refraction stack on or the high-incidence reflection stack has not been investigated: it might be explained by the mute design before stack, too wide on both stacks, erroneous statics and excessive lateral mixing.
- A series of step faults of the base of ophiolite, located in the interval between CMP #4500 and 4000, expresses the deepening of the ophiolite layer westwards: the interval between the green marks appears as a wide accident zone on the refracted arrivals of shot collections. The width of the mute before stack tends to smooth out this series of step fault accidents clearly marked by plums on the refraction stack base ophiolite horizon on Fig. 10a (top display).

Discussion

- Data quality of the deep seismic survey, field acquisition

The quality of the acquired data, regarding the criterions of high source energy, long offsets, consistence of the seismic acquisition quality along the line, limitation of slaloming turns, is particularly appreciable for the reliability of the processed results at large offsets. Additionally to vibroseis acquisition, a few powerful quarry blasts, several tonnes of explosives each, were recorded on all the seismic channels connected at the moment of the explosions, using the radio links available on the WesternGeco field crew.

- How could the seismic image below the ophiolite top be improved?

Building a CMP-refraction stack from the raw shot collection, without mute and with appropriate deconvolution of the first arrivals would certainly be desirable over the ophiolite outcrops. The results from a computerised Gardner refraction processing method and from an improved refraction stack-processing procedure would be highly desirable as a seismic exploration approach for mapping the base of the ophiolite layer. Some limited R&D effort could be devoted to this approach.

Building a CMP reflection stack in ONE PASS looks now feasible using any industrial seismic software, according to the encouraging results obtained on test line D1: the one-pass reflection stack would include the low to medium incidence top ophiolite reflection over the Tertiary cover, as performed by the contractor, as well as the high sub-critical incidence reflection of the base ophiolite, as long as sufficient attention is devoted to the definition of the mute and stacking domain of the base ophiolite reflection. For the deep sub-ophiolite reflections down to 5 s twt, the high-incidence of reflection stack might reveal additional events, as the stacking velocities can be better constrained, and as

long as multiple arrivals can be identified and eliminated from the reflection stack.

The refraction stack confirms the ~6 km/s velocity below the reflective interface at the ophiolite base. At present, the analysis of the headwave refraction arrivals, including the examination of single-shot collection records, is more appropriate to the fine definition of geological accidents, as long as near-critical refraction stacking methods are not properly industrialised. However, the refraction stack approach in the immediate vicinity of the critical incidence offers a fast imaging solution which can be further improved.

The result of high-incidence reflection stacking is directly in two-way times, while intercept refraction times need to be converted to vertical times. This promising test opens the door to a one-pass reflection stack-imaging procedure for the whole section.

Where the ophiolite is under sedimentary cover, the reflection from the base ophiolite appears sporadically even on the near-offset data, so that the near-offset reflectivity value must be very weak, but not null everywhere.

- Seismic signature of Fault F3 intersected by line D1 at CMP #5850 (STN #4970, and Fault F4 at CMP #6010; STN #5060)

A significant accident, noted F3 on Figs. 3a, 4, 6, 12 and 13, can clearly be seen on refraction first arrivals, in association with a notable change of refraction marker, deeper in the eastern fault compartment. The vibroseis records displayed on Fig. 13, in reduced time (LMO corrected) with the same receiver spread, clearly show the F3 accident at station STN #4970 for both shallow and deep refraction markers; the field position of this event is invariant with the shot position, which confirms the presence of a major accident at this location (field station STN #4970, or CMP #5850). On the quarry blast record #2269 (Fig. 6), the accident F3 can be seen as a change

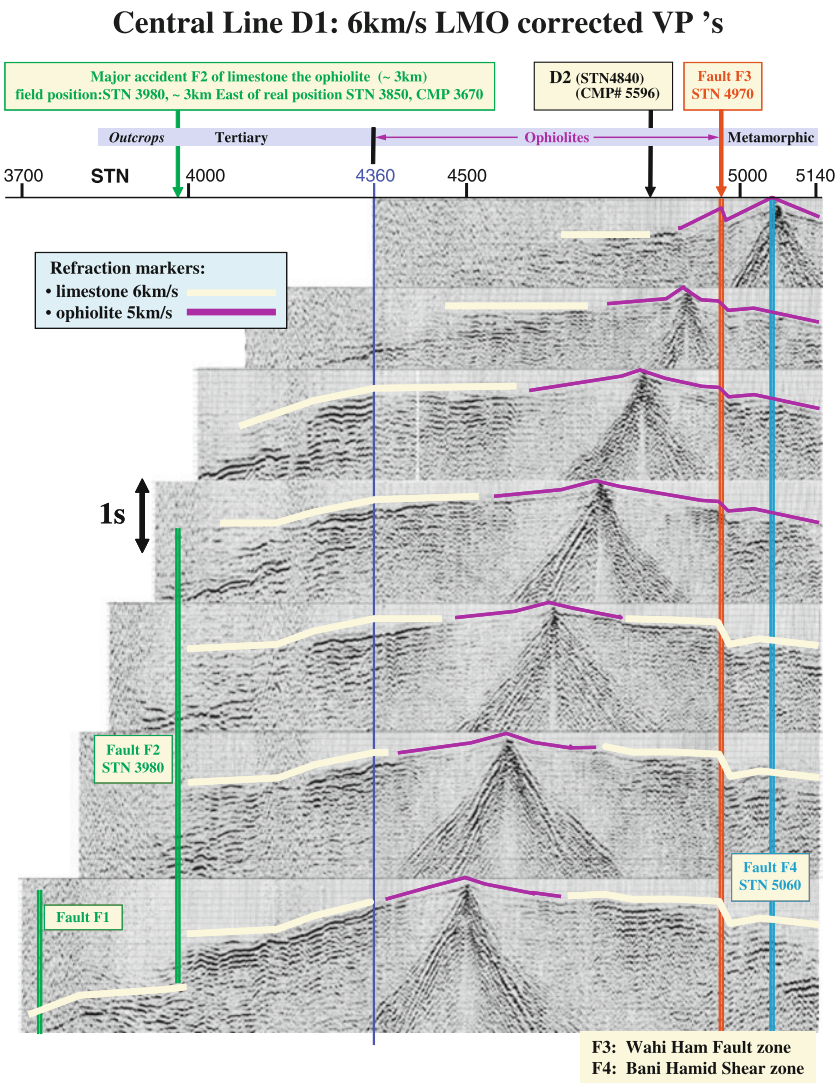

Fig. 13 Central line D1: 6 km/s corrected VPs, evidencing major refraction accidents

of marker, with a faint forerunner signal, associated with a thin ophiolite superficial layer, present on the west side of F3, absent on the eastern side.

Further east, at field station STN #5060, or CMP 6020, a major deep accident (F4) clearly appears on Fig. 6; the same refraction response pattern can be observed on the two vibroseis records displayed at the bottom of Fig. 13, located at STN #4490 and 4510, and vibroseis shot VP #4500 (Fig. 4, bottom), located father west from the F3–F4 accidents than the projected position of quarry blast #2269, near STN 4700 (Fig. 3). Note that fault F4 is observed in field position STN #5060, and corresponds to the apparition of deep refraction markers on its eastern compartment (ex: 1.8s on right end of Fig. 6); therefore, if replaced in true position, at a distance of one refraction offset distance closer to the source, accident F4 would be located near the position of fault F3. In other words, the accidents F3 and F4 may correspond to the same accident observed at different depths, corresponding to the Wahi Ham fault zone, illustrated by the map enlargement Fig. 15.

The superficial marker change marked by Fault F4 corresponds to the eastern edge of the Wadi Ham Fault zone (Figs. 3a and 15), intersecting at the same location the Bani Hamid shear zone (Styles et al. 2006; Goodenough et al. 2010). Nevertheless, the deeper marker(s) evidenced at about the same field position F4 are related mainly to the Wadi ham fault zone

Fault F3 corresponds to the western edge of the Wadi Ham Fault Zone, associated with an aero-magnetic accident, and marked by an abrupt change of outcrop lithology, from ophiolite to metamorphic, west to east (Figs. 1, 3a, 4, 13 and 15), locally aligned with the NW–SE magnetic accident along the river flowing from Masafi down to Fujairah on the ocean coast.

The near-critical refraction and reflection stacks (Figs. 10 and 12) unfortunately show no obvious sign of fault F3, possibly due to a too large offset range domain retained before stacking, resulting in a highly lateral mixing of the seismic result near-critical angle, and possible annihilation of the F3 fault throw by application of the static corrections computed by WesternGeco, using refraction tomography! This observation suggests that both refraction and reflection stacking procedures definitely need to be improved, and completed by a sound direct-refracted arrival analysis.

Last, the near critical refraction/reflection marker is not well identified: this point alone would justify additional seismic processing, analysis and interpretation using external information when available.

- AVO effects at the base of ophiolite interface.

In order to fully characterise the interface of the base ophiolite (5 km/s) with the underlying top limestone (6 km/s), separated by a thin metamorphic layer (possibly 5 km/s ?), an AVO simulation of the base of ophiolite interface has been performed using Zoeppritz equations:

On Fig. 14, where ophiolite density is 3.0, sub-ophiolite formation density is 2.6, the reflection coefficient curve (red) clearly illustrates how the P–P reflection coefficient of the base ophiolite interface can be quite null at low to zero incidence, then suddenly increases beyond 50°, reaching a peak at the 58° critical incidence.

Therefore, the very weak reflection observed on the seismic stack indicates that the ophiolite density value should range from about 2.9 to 3.0 gr/cc, with 2.6 gr/cc (or a bit less?) for the underlying limestone.

Actually, some density measurements of rock samples selected on weathered outcrops and in local quarries have been performed by BGS in late 2009, suggesting that the density of the basal ophiolites and metamorphic sole rocks could reasonably reach values between 2.7 and 3.0 gr/cc, as long as they are not highly fractured. These observations tend to confirm the existence of a negative density contrast

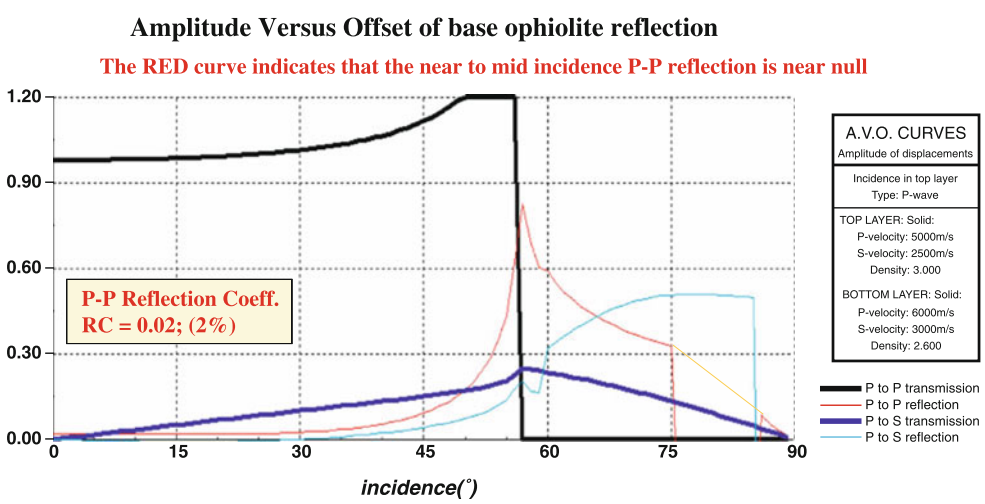

Fig. 14 Amplitude versus offset of base ophiolite reflection by Zoeppritz simulation

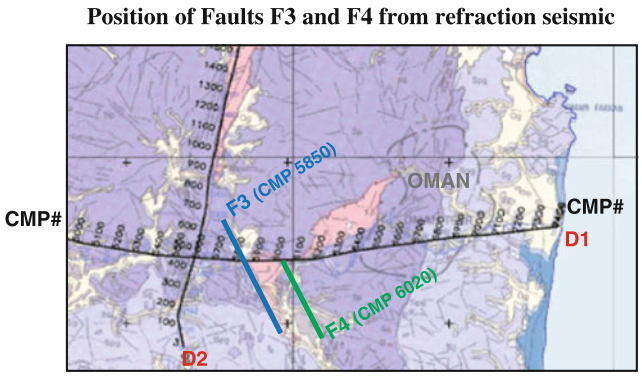

Fig. 15 Position of faults F3 and F4 from refraction seismic, on enlarged geological map

at the base of metamorphic sole with the underlying limestone, opposite to the positive velocity contrast deduced from refraction seismic at the same interface.

Very likely, the main contrast accounting for the near-critical reflection would be located at the top of the limestone underlying the Semail ophiolite, basal metamorphic, and mantle rock sole: however, this best guess need to be confirmed, as the 700 m estimated thickness value of ophiolite outcrop of 700 m at the D1/D2 line crossing looks quite high (Figs. 12 and 15). Taking in account that the ophiolite outcrops are totally eroded at Masafi, a few kilometres the North, laterally to line D1, the value of the southern downdip of the ophiolite base between Masafi to line D1 may or may not be plausible if the observed refraction marker is identified as the ophiolite base, with respect to external structural considerations.

Additional information from shallow water wells in the Masafi area would be welcome to refine the seismic response and interpretation of the base ophiolite interface.

Apatite fission tracks and dating of the unroofing episodes

Numerous ~95-Ma-old plagiogranites plug the Semail Ophiolite (Searle and Cox 2002) and were recently mapped by BGS within the Emirati part of the Semail Ophiolite, both near the current erosional top of this unit near Fujjairah, and near the sole thrust of this unit, in the core of the Masafi nappes anticline (Phillips et al. 2006; Styles et al. 2006; Goodenough et al. 2010). Zircons and other heavy minerals extracted and separated for the purpose of radiometric dating of these plutons, were also helpful for controlling the timing of tectonic uplift and unroofing of the ophiolite.

Two samples (UAE 164 and 169) collected in a late magmatic suite in the easternmost and uppermost part of the ophiolite near Fujairah (Fig. 1) yielded very old (72.6±11.0 and 76.4±12.8 Ma, respectively), Cretaceous ages of unroofing, which are indeed consistent with the occurrence of continental deposits and shallow water rudist-bearing reefal series along the western side of the ophiolitic complex (Woodcock and Robertson 1982; Hamdan 1990). This implies that the ophiolite was already deeply eroded during its tectonic transport, piggyback of the Hawasina-Sumeini accretionary wedge, a long time before it reached its current structural position on top of the Arabian Platform.

Sample UAE 178 was collected in a metagabbro the core of the Masafi window, very close from the base of the Semail ophiolite, and provided a Neogene age (20.3± 3.2 Ma), which agrees with the young age proposed for the thick-skinned tectonic accretion of the Arabian basement at the inner base of the tectonic pile (Figs. 2 and 16) accounting for the refolding of overlying allochthonous nappes (made up of the Hawwasina-Sumeini units, as well as the metamorphic sole and overlying Semail Ophiolite).

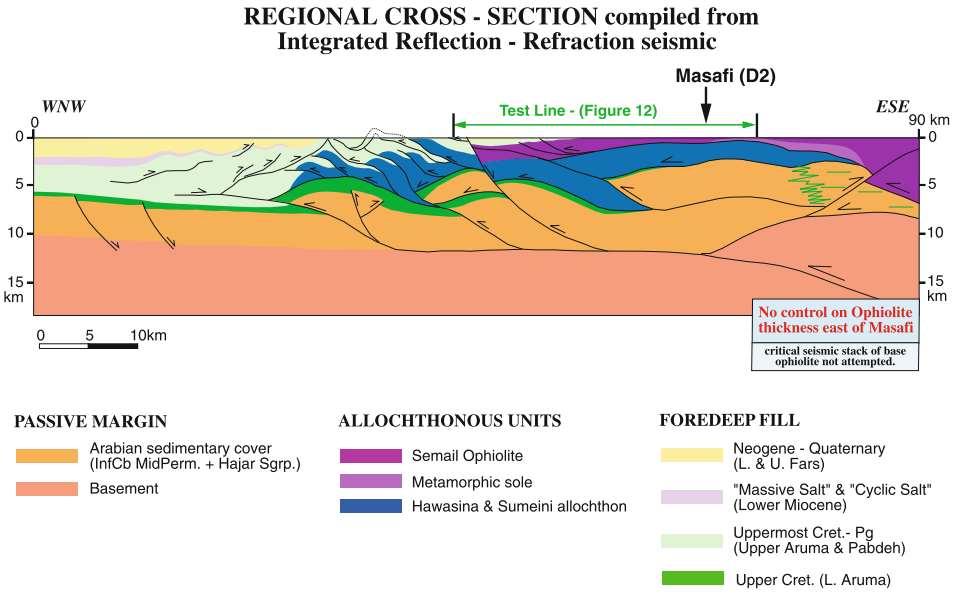

Fig. 16 Structural interpretation of profile D1, based on the depth-converted reflection profile. The Semail Ophiolite is in *purple*, the Hawasina-Sumeini allochthon in *blue*, and the foreland Arabian platform and coeval parautochthonous units in *orange*, with the uppermost (Lower Cretaceous) reservoirs in *green*

A single site (UAE 180) provides an intermediate, Paleogene (40.6±3.9 Ma) ages. This intermediate age of unroofing could (1) relate to a partial resetting of the apatites in the vicinity of active hot fluid conduits, as the sample locality is close to a major NW trending tear fault dissecting the Semail Ophiolite, (2) derive from a continuous and slow unroofing of the ophiolite occurring between the time of its Late Cretaceous obduction episode and the time of its passive refolding during the Neogene, or (3) indicate a reactivation of the Wadi Ham fault (F3) during the Paleogene.

Because these FT ages are likely to record the cooling age when individual rock samples crossed the 100 or 110°C isotherm, they provide further constraint on the maximum thickness of the ophiolite in the Masafi area, which was already less than 3 km since the onset of the Miocene folding and unroofing, assuming an average geothermal gradient of about 30°C/km.

Conclusions and suggestions

The base of the Semail ophiolite layer has been tracked for the first time by industrial seismic profiling and adapted industrial seismic-processing procedure.

The refraction and high-incidence reflection stacks obtained in slightly different near-critical offset ranges definitely demonstrate the technical capability of the seismic technique to map the base of ophiolite in the eastern UAE region.

Enhancing the seismic image quality of the ophiolite base could be attained with moderate industrialisation efforts aiming to a one-pass reflection stack-imaging procedure for the whole section. Appropriate QC controls and optimisation tools can be designed within the existing commercial seismic processing software.

On one hand, it would be desirable that the seismic industry revisits the refraction and wide angle and critical incidence reflection methods of seismic imaging, for exploring the areas where standard seismic reflection fails.

On the other hand, some academic institutions should be encouraged to implement new approaches for processing and interpreting the refraction data, not only the most sophisticated ones like full wave inversion, but also the old basic methods of refraction processing.

The west-dipping attitude of the basal contact of the Semail ophiolite west of the Masafi tectonic window is in good agreement with the predictive sections built before the deep seismic acquisition, and results from a late stage refolding of the far-travelled basinal allochthon (i.e., Semail +Hawasina-Sumeini accretionary complex) during the duplexing of underlying Arabian Platform, which developed during the Neogene.

Because the north-trending profile D2 was shot parallel to the axis of the Masafi tectonic window, this profile help evidencing a thick sedimentary pile still preserved beneath the Semail Ophiolite in the inner part of the Oman Range. However, in the lack of deep wells there, it is not yet possible to demonstrate whether the lower plate units are made up of dominantly far travelled units such as the Hawasina and Sumeini allochthon, or if it also involves the platform series of the former Arabian passive margin, as what is currently observed in the wide tectonic windows of Oman (Jebel Akhdar; Breton et al. 2004).

No attempt was made within the frame of this study to process the long offset traces of the eastern part of D1 (east of Masafi), thus no information is available at present time about the ophiolite thickness along the eastern part of this transect.

Following the encouraging results obtained so far on test line D1, the authors suggest carrying out improved refraction and near-critical reflection-processing procedures on the eastern seismic profiles of the present study area:

- on line D2 in order to tentatively identify the strong near-critical angle reflecting interface, either the base ophiolite or the base metamorphic sole, or the base of the near surface decompressed and weathered zone (?), as line D2 crosses the outcropping limit of both top and base of metamorphic sole interfaces.
- on the eastern part of D1 and D4 lines, in order to better define the depth of the base ophiolite.

Acknowledgments We acknowledge Saleh Al Mahmoudi, Khalid Al Hosani, Abdullah Gahnoog and the Ministry of Energy of the UAE for their long-term support during this project and authorising this publication. Drs. M Styles and QG Crowley, from BGS, extracted and provided us the apatite grains from the plagiogranites. Andy Chadwick and John Rowley of BGS, supervised the field operations. Graham Milne and his W-G processing centre colleagues Francis Malcom, Dave Rose, Nigel Sayer, provided access to all geophysical field data used during this study. Special thanks to the field operation supervisor and engineers, Andrew SJ Sewell, Paul West and all their colleagues of the WesternGeco seismic field crew, for their efficient collaboration and for the high quality of the acquired data.

References

Alsharhan AS (1989) Petroleum geology of the United Arab Emirates. Jour Petrol Geol 12:253–288

Blinton JS, Wahid IA (1983) A review of Sajaa field development, Sharjah. United Arab Emirates, 3rd Middle East Oil Show, SPE Bahrain, 601–606

Breton JP, Béchennec F, Le Métour J, Moen-Maurel L, Razin P (2004) Eoalpine (Cretaceous) evolution of the Oman Tethyan continental margin: insights from a structural field study in Jabal Akhdar (Oman Mountains). GeoArabia 9(2):41–58

Callot JP, Breesch L, Guilhaumou N, Roure F, Swennen R, Vilasi N (2010) Paleo-fluid characterization and fluid flow modelling

along a regional transect in the Northern Emirates, doi:10.1007/s12517-010-0233-z
Clément A, Layat C (1961) Corrélation à distance constante en sismique réfraction, EAGE 19th meeting, Paris, 1–9 Dec 1960, 296–305
Coleman RG (1981) Tectonic setting for ophiolite obduction in Oman. Jour Geophys Res 86:2497–2508
Gardner LW (1939) An areal plan of mapping subsurface structure by refraction shooting. Geophysics 4:247–359
Ghent ED, Stout MZ (1981) Metamorphism at the base of the Samail ophiolite, southeastern Oman Mountains. Jour Geophys Res 86:2557–2571
Gnos E, Peters T (1993) K-Ar ages of the metamorphic sole of the Samail Ophiolite: implications for ophiolite cooling history. Contrib Mineralog Petrol 113:325–332
Goffé B, Michard A, Kienast JR, Le Mer O (1988) A case of obduction-related high pressure, low temperature metamorphism in upper crustal nappes, Arabian continental margin, Oman: P–T paths and kinematic interpretations. Tectonophysics 151:363–386
Goodenough K, Styles MT, Schofield DI, Thomas RJ, Crowley QG, Lilly RM, McKervey J, Stephenson D, Carney J (2010) Architecture of the Oman-UAE Ophiolite: evidence for a multi-phase magmatic history, doi:10.1007/s12517-010-0177-3
Gray DR, Gregory RT (2000) Implications of the structure of the Wadi Tayin metamorphic sole, the Ibra-Dasir block of the Semail ophiolite, and the Saih Hatah window for a late extensional ophiolite emplacement, Oman. Mar Geophys Res 21:211–227
Gray DR, Gregory RT, Miller JM (2000) A new structural profile along the Muscat-Ibra transect, Oman: implications for emplacement of the Semail ophiolite. Geol Soc Am Spec Paper 349:513–523
Hamdan ARA (1990) Maastrichtian Globotruncanids from the western front of the northern Oman Mountains: implications for the age of post-orogenic strata. J Fac Sci United Arab Emirates Univ 2:53–66
Lanphere MA (1981) K-Ar ages of metamorphic rocks at the base of the Semail Ophiolite. Jour Geophys Res 86:2777–2782
Layat C (1967) Modified "Gardner" delay time and "Constant Distance Correlation" interpretation. In Musgrave AW (ed) Seismic Refraction Prospecting, 171–193
Le Métour J, Rabu D, Tegyey M, Béchennec F, Beurrier M, Villey M (1990) Subduction and obduction: two stages in the Eo-Alpine tectonometamorphic evolution of the Oman Mountains. In Robertson AHF, Searle MP, Ries CA (eds) The geology and tectonics of the Oman region, Geol. Soc., London, Spec. Publ., 49, 327–341
Lippard SJ (1983) Cretaceous high pressure metamorphism in NE Oman and its relationship to subduction and ophiolite nappe emplacement. J Geol Soc Lond 140:97–104
Michard A, Goffé B, Ouazzani-Touhami M (1982) Obduction-related high pressure-low temperature metamorphism in upper crustal materials, Muscat, Oman. Terra Cognita 3:187
Ministry of Energy of the UAE (2006) Reports on FUGRO airborne magnetic and radiometric surveys consisting of 10 volumes and 120 maps and images
Muceku B, Mascle GH, Tashko A (2007) First results of fission-track thermochronology in the Albanides. Geol Soc London, Spec Publ 260:539–556
Naville C, Girard F, Ancel M (2006) Deep seismic survey in the Northern Emirates. Part IV- refraction seismic report: lines D1, D2, D4. Ministry of Energy, UAE-IFP Report n° 59361, 25 p + Figures
O'Donnell GP, Daly CB, van Mount S, Krantz RW (1994) Seismic modelling over the Margham field, Dubai, United Arab Emirates. In Al Husseini MI (ed) GEO'94, The Middle East Petroleum Geosciences, Bahrain, April 1994, II, 737–746
Péraldi R, Clément A (1972) Digital processing of refraction data—study of first arrivals. Geophys Prospect 20:529–548
Phillips ER, Ellison RA, Farrant AR, Goodenough KM, Arkley SLB, Styles MT (2006) Geology of the Dibba 1:50,000 map sheet, 50-2, United Arab Emirates. British Geological Survey, Keyworth, 59 pp
Rabu D (1987) Géologie de l'autochtone des Montagnes d'Oman: la fenêtre du Jabal Akhdar. La semelle métamorphique de la nappe ophiolitique de Samail dans les parties centrale et orientale des Montagnes d'Oman: une revue. PhD Thesis, Univ. P. et M. Curie, Documents du BRGM, Orléans, France, 130 p
Roure F, Andriessen P, Breesch L, Broto K, Bruneau J, Chérel L, Collin M, Ellouz N, Faure JL, Guilhaumou N, Jardin A, Muller C, Naville C, Ricarte P, Rodriguez S, Swennen R, Tarapoanca M (2006) Deep seismic survey in the Northern Emirates, Part II: Main interpretation and modelling report. Ministry of Energy, UAE-IFP Report n° 59 359, 125 p
Roure F, Andriessen P, Callot JP, Ferket H, Gonzales E, Guilhaumou N, Hardebol N, Lacombe O, Malandain J, Mougin P, Muska K, Ortuño S, Sassi W, Swennen R, Vilasi N (2010a) The use of paleo-thermo-barometers and coupled thermal, fluid flow and pore fluid pressure modelling for hydrocarbon and reservoir prediction in fold and thrust belts. Geological Society, London (in press)
Roure F, Cloetingh S, Scheck-Wenderoth M, Ziegler P (2010b) Achievements and challenges in sedimentary basins dynamics. In Cloetingh S, Negendank J (eds) New Frontiers in integrated solid Earth Sciences, International Year of Planet 145 Earth, doi:10.1007/978-90-481-2737-5_5
Searle M, Cox J (1999) Tectonic setting, origin and obduction of the Oman Ophiolite. Geol Soc Am Bull 111(1):104–122
Searle MP, Cox JS (2002) Subduction zone metamorphism during formation and emplacement of the Semail Ophiolite in the Oman mountains. Geol Mag 139(3):241–255
Searle MP, Malpas J (1980) The structure and metamorphism of rocks beneath the Semail Ophiolite of Oman and their significance in ophiolite obduction. Trans R Soc Edinb Earth Sci 71:213–228
Searle MP, Malpas J (1982) Petrochemistry and origin of sub-ophiolitic metamorphic and related rocks in the Oman Mountains. Jour Geol Soc Lond 139:235–248
Styles MT, Ellison RA, Arkley SLB, Crowley Q, Farrant A, Goodenough KM, McKervey JA, Pharaoh TC, Phillips ER, Schofield D, Thomas RJ (2006) The geology and geophysics of the United Arab Emirates. British Geological Survey, Keyworth
Tarapoanca M, Andriessen P, Broto K, Chérel K, Ellouz-Zimmerman N, Faure JL, Jardin A, Naville C, Roure F (2010) Forward kinematic modelling of a regional transect in the Northern Emirates, using apatite fission track age determinations as constraints on paleo-burial history, doi:10.1007/s12517-010-0213-3
Woodcock NH, Robertson AHF (1982) Stratigraphy of the Mesozoic rocks above the Semail Ophiolite, Oman. Geol Mag 119:67–76